The EMBO Journal (2006) 25, 2802–2813 | © 2006 European Molecular Biology Organization | All Rights Reserved 0261-4189/06
www.embojournal.org

THE EMBO JOURNAL

Dose-dependent effects of stable cyclin B1 on progression through mitosis in human cells

Frank Wolf, Cornelia Wandke, Nina Isenberg and Stephan Geley*

Division of Molecular Pathophysiology, Biocenter, Innsbruck Medical University, Innsbruck, Austria

The disassembly of the mitotic spindle and exit from mitosis require the inactivation of Cdk1. Here, we show that expression of nondegradable cyclinB1 causes dose-dependent mitotic arrest phenotypes. By monitoring chromosomes in living cells, we determined that pronounced overexpression of stable cyclinB1 entailed metaphase arrest without detectable sister chromatid separation, while moderate overexpression arrested cells in a pseudometaphase state, in which separated sister chromatids were kept at the cellular equator by a bipolar 'metaphase-like' spindle. Chromosomes that left the pseudometaphase plate became pulled back and individual kinetochores were found to be merotelically attached to both spindle poles in stable cyclinB1 arrested cells. Inactivation of the chromokinesin hKid, by RNAi or antibody microinjection, prevented the formation of stable bipolar spindles and the 'metaphase-like' alignment of chromosomes in cells expressing stable cyclinB1. These experiments show that cyclinB1 is able to maintain a bipolar spindle even after sister chromatids had become separated and suggest an important role of hKid in this process. Cells expressing low levels of nondegradable cyclinB1 progressed further in mitosis and arrested in telophase.

The EMBO Journal (2006) **25,** 2802–2813. doi:10.1038/sj.emboj.7601163; Published online 25 May 2006
Subject Categories: cell cycle
Keywords: anaphase; chromokinesin; cyclin; hKid; mitosis; proteolysis

Introduction

In all organisms studied, cyclin degradation is essential for completion of mitosis, but a detailed understanding of why nondegradable cyclinB1 blocks exit from mitosis is still lacking. During interphase, cyclinB1, the main mitotic cyclin in human cells, associates with Cdk1 in an inactive complex until it becomes activated to trigger entry into mitosis. At the onset of anaphase, cyclinB1 becomes degraded in a polyubiquitylation-dependent manner, which is mediated by the ubiquitin ligase 'anaphase promoting complex/cyclosome (APC/C)'. In addition to cyclinB1, the APC/C also controls the proteolysis of the anaphase inhibitor securin and is thus essential for anaphase and exit from mitosis (Peters, 2002). To prevent chromosome gain or loss during mitosis, sister chromatid separation and exit from mitosis are controlled by the spindle assembly checkpoint, which guarantees that cells do not progress beyond metaphase until all chromosomes have achieved bipolar attachment (Chan and Yen, 2003). The spindle assembly checkpoint inhibits the APC/C and, thus, protects sister chromatid cohesion and keeps cells in mitosis by maintaining high cyclin/CDK activity. Once all chromosomes have become attached to the mitotic spindle in a bipolar manner, the checkpoint-mediated inhibition of the APC/C is released and the degradation of securin and cyclinB1 commences at the same time (Clute and Pines, 1999; Hagting *et al*, 2002). Once sister chromatid cohesion has been removed, the pulling forces of the mitotic spindle can act on kinetochores to tear the two sister chromatids apart (Nasmyth, 2001b). Although cyclin B1 is degraded concomitantly with securin, it is not clear whether this timing of cyclinB1 proteolysis is important since the mitotic processes that require cyclinB1 inactivation are poorly understood.

Securin inhibits separase (Waizenegger *et al*, 2002), a cysteine protease that is essential to resolve the physical linkage between the sister chromatids by cleaving the cohesin subunit Scc1/Mcd1/Rad21. While overexpression of nondegradable securin prevented anaphase (Zur and Brandeis, 2001; Hagting *et al*, 2002), loss-of-function did not cause precocious sister chromatid separation in human cells (Jallepalli *et al*, 2001), suggesting additional layers of anaphase control. Recently, two additional mechanisms have been identified that contribute to the regulation of anaphase. Firstly, maintenance of centromeric sister chromatid cohesion requires Sgo1, since RNAi-mediated protein knockdown of Sgo1 causes premature sister chromatid separation during prometaphase (Salic *et al*, 2004; McGuinness *et al*, 2005) and secondly, separase activity can be controlled by cyclinB1/Cdk1.

To delineate the role of cyclinB1 degradation, Stemmann *et al* (2001) investigated the effects of nondegradable cyclinB1 and found that sister chromatid separation is affected by cyclinB1 in a dose-dependent manner *in vitro*. High levels of nondegradable cyclinB1 (but not physiological levels (Holloway *et al*, 1993)) caused the inhibition of separase and prevented sister chromatid separation in cell-free *Xenopus* egg extracts. This inhibitory effect is caused by Cdk1-dependent phosphorylation of, and direct cyclinB1/Cdk1 binding to, separase (Gorr *et al*, 2005). However, although confirmatory observations were reported in mouse oocytes (Herbert *et al*, 2003; Madgwick *et al*, 2004), the proposed role of cyclinB1 proteolysis in controlling sister chromatid separation in mitosis is more controversial.

Expression of nondegradable chicken cyclinB2 in HeLa cells caused a mitotic arrest with condensed chromosomes in a pseudomitotic state and multipolar spindles (Gallant and Nigg, 1992). Expression of nondegradable sea urchin cyclinB

*Corresponding author. Division of Molecular Pathophysiology, Biocenter, Innsbruck Medical University, Fritz-Pregl-Str. 3, 6020 Innsbruck, Austria. Tel.: +43 512 507 3103, Fax: +43 512 507 2867; E-mail: stephan.geley@i-med.ac.at

Received: 12 August 2005; accepted: 2 May 2006; published online: 25 May 2006

in normal rat kidney (NRK) cells, however, caused cells to arrest in telophase (Wheatley *et al*, 1997). Again, different results were obtained with expression of GFP-fusion proteins of nondegradable human cyclinB1 in rat kangaroo and HeLa cells, which arrested cells in ana- and metaphase, respectively (Hagting *et al*, 2002; Chang *et al*, 2003).

The results obtained in these studies are difficult to compare with each other for several reasons. First, different expression technologies have been used for expressing nondegradable B-type cyclins, for example, microinjection of *in vitro* transcribed RNA or transient transfection of cDNA expression plasmids, which might lead to substantial differences in expression levels. Only two studies have quantified the expression levels of the nondegradable cyclinB but arrived at different conclusions. Hagting *et al* (2002) found that only high levels of nondegradable cyclinB1 could block the onset of anaphase, whereas Chang *et al* (2003) claimed that nondegradable cyclinB1 expressed at 30% of the endogenous level was sufficient to block anaphase. Second, the above studies employed different nondegradable versions of B-type cyclins of different species and with different stabilising mutations, which also might cause some confounding effects.

To overcome some of the technical limitations of the previous approaches, we generated a conditional expression system for nondegradable cyclinB1 in a human cell line and quantified the induced nondegradable cyclinB1 levels on a single cells basis. In combination with time-lapse videomicroscopy to monitor chromosome behaviour during mitosis, we found that nondegradable cyclinB1, at levels roughly equivalent to the endogenous levels, does not block sister chromatid separation but maintains a stable bipolar spindle able to keep anaphase chromosomes in a metaphase-like plate.

Results

Nondegradable cyclinB1 arrests human cells in a 'metaphase-like' state

To study the effects of maintaining high Cdk1 activity during mitosis, we generated several human cell lines with tetracycline-inducible expression of mouse cyclinB1 (mB1), and the nondegradable mutants mB1NΔ157 and mB1dm, which lack the N-terminal 157 amino-acid residues, including the destruction box (D-box, residues 42–50) or carry two point mutations (Arg42 and Leu45 to Ala), which render the D-box nonfunctional, respectively (for details see Supplementary data). Throughout all experiments, both cell systems (mB1dm and mB1NΔ157) gave similar results.

We first generated human osteosarcoma-derived cell lines (Onk2; Geley *et al*, 2001) with conditional expression of untagged mouse cyclinB1 and its mutants. As shown in Figure 1A, upon addition of 400 ng/ml doxycycline (dox), transgenic mB1dm at 24 h after induction was expressed at levels ~3 times higher than endogenous cyclinB1. This led to an accumulation of rounded-up mitotic cells with condensed chromatin in an apparent 'metaphase-like' state (Figure 1B). To be able to follow cyclinB1 induction and quantify its levels in individual cells, we also generated cell lines with GFP-tagged cyclinB1 mutants. GFP-tagged mB1dm was detectable at peak levels 8 h after induction (Figure 1C). To relate the expression levels of the mutants to endogenous cyclinB1

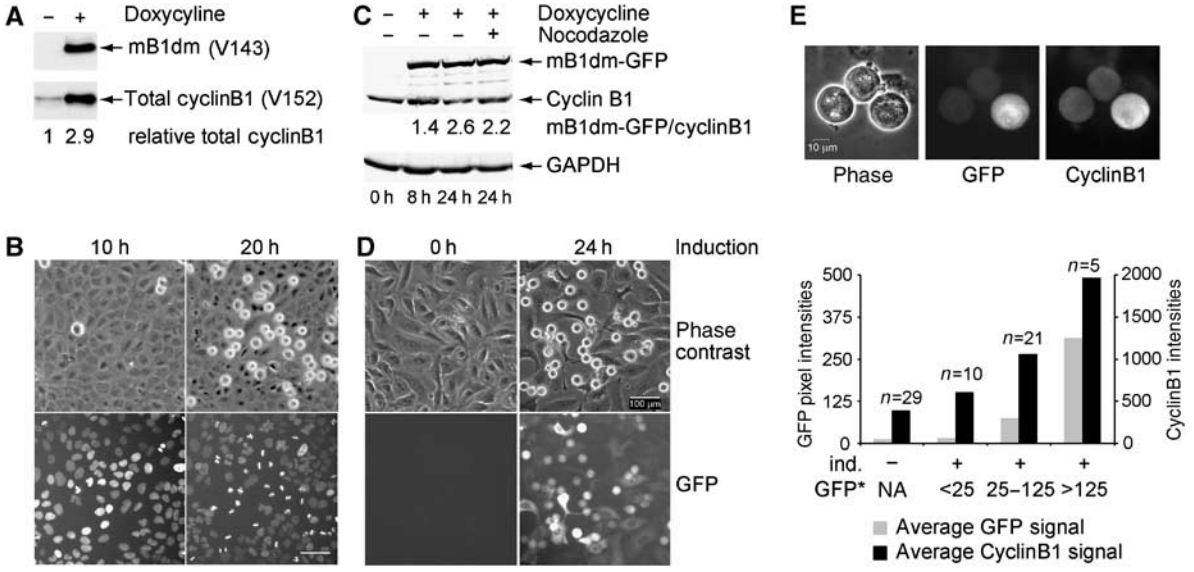

Figure 1 Nondegradable cyclinB1 arrests cells in mitosis. (**A**) Onk2H2B-GFP-mB1dm cells were induced for 24 h using 400 ng/ml dox and analysed for cyclinB1 expression using mouse-specific mAb V143 and V152 that recognises both mouse and human cyclin B1. The mB1dm expression level in relation to endogenous cyclin B1 as determined by densitometry of the autoradiograph is depicted underneath the blots. (**B**) Phase contrast and fluorescence images were taken at 10 and 20 h after induction of Onk2-H2B-GFP mB1dm cells. (**C**) Onk2-mB1dm-GFP cells were treated with 400 ng/ml dox (lanes 2–4) and 500 nM nocodazole for 16 h (lane 4). Total protein extracts were analysed for cyclinB1 expression at the indicated time points after induction using mAb V152, detected and quantified using an infrared scanner. (**D**) Phase contrast and fluorescence (mB1dm-GFP) images were taken at 0 and 24 h after induction. (**E**) mB1dm-GFP cells induced for 24 h and treated with nocodazole for 16 h were fixed with paraformaldehyde, permeabilized and stained for cyclinB1 using mAb V152. Panels show phase contrast, GFP fluorescence and cyclinB1 immunofluorescence images and a quantification of GFP fluorescence and cyclinB1 immunofluorescence pixel intensities/cell. Cells were classified according to GFP signals (GFP*, NA = not applicable in noninduced cells) and average GFP signals plotted against average cyclinB1 pixel intensities.

levels, dox-induced cells were treated with nocodazole to prevent the degradation of endogenous cyclinB1, which revealed that mB1dm-GFP accumulated to 2.2-fold higher levels than endogenous cyclinB1 (Figure 1C, last lane). More than 90% of induced cells became GFP positive and ~50% became arrested in mitosis; however, differences in individual GFP intensities were observed (Figure 1D).

To evaluate cyclinB1 levels in individual cells, mB1dm-GFP cells were induced using dox and, 8 h after induction, nocodazole was added for 16 h prior to immunostaining of mitotic cells for cyclinB1 protein. This treatment caused induction of mB1dm-GFP and prevented the degradation of endogenous cyclin B1 (see below), allowing us to compare the expression of transgenic nondegradable cyclin B1 with that of endogenous cyclin B1 at its peak at metaphase of mitosis. As shown in Figure 1E, mitotic cells with low GFP signals (average pixel intensity per cell after background correction = 25) had cyclinB1 levels similar to noninduced cells, while cells with higher levels (25–125 pixel intensities) displayed total cyclin levels that were about twice the endogenous levels. The highest mB1dm-GFP expressing cells (>125 pixel intensities, max = 434) reached about three- to four-fold elevated total cyclinB1 levels. Thus, in the majority of induced mitotic cells (58%), nondegradable cyclinB1 accumulated to levels that were comparable to the endogenous cyclinB1 levels of nocodazole-arrested cells. Similarly, induction of Onk2-mB1NΔ157 cells caused an accumulation of nondegradable cyclins to levels that were only slightly higher (see Supplementary Figure S1) than the endogenous cyclin B1 in nocodazole arrested cells.

Analysis of chromosome movements in cells expressing nondegradable cyclin B1 defines three mitotic arrest phenotypes

To obtain a more detailed insight into the arrest phenotype induced by nondegradable cyclinB1, we performed fluorescence time-lapse video microscopy in induced Onk2-H2B-GFP-mB1NΔ157 cells to monitor the behaviour of GFP-labelled chromatin. Cells were synchronised and induced to express nondegradable cyclinB1 during the second thymidine block and subsequent release. This protocol allowed the analysis of several hundred arrested cells by time-lapse video microscopy with phase contrast and fluorescence images taken every 2.5–5 min. During the observation period, ~50% (34–56% depending on synchronisation efficiency) of the observed cells arrested in mitosis. In cells undergoing normal mitosis, prometaphase, scored as the time from visible chromosome condensation to chromosome alignment at the metaphase plate, lasted approximately 15–20 min, metaphase 10–20 min and completion of mitosis, that is, anaphase to chromosome decondensation, again 15–20 min.

The majority of arrested cells (93%, $n = 568$) exhibited one of three phenotypes, while 7% displayed other, more irregular, phenotypes. Figures 2 and 3 show individual frames of selected cells representing the three mitotic arrest phenotypes in cells expressing mB1NΔ157. In the most frequently observed phenotype, 48% of mitotic cells became arrested in a 'pseudometaphase' state. Like control cells, induced cells entered mitosis about 10 h after the release from the second thymidine block and progressed until metaphase with normal kinetics. At the expected timing for the meta-

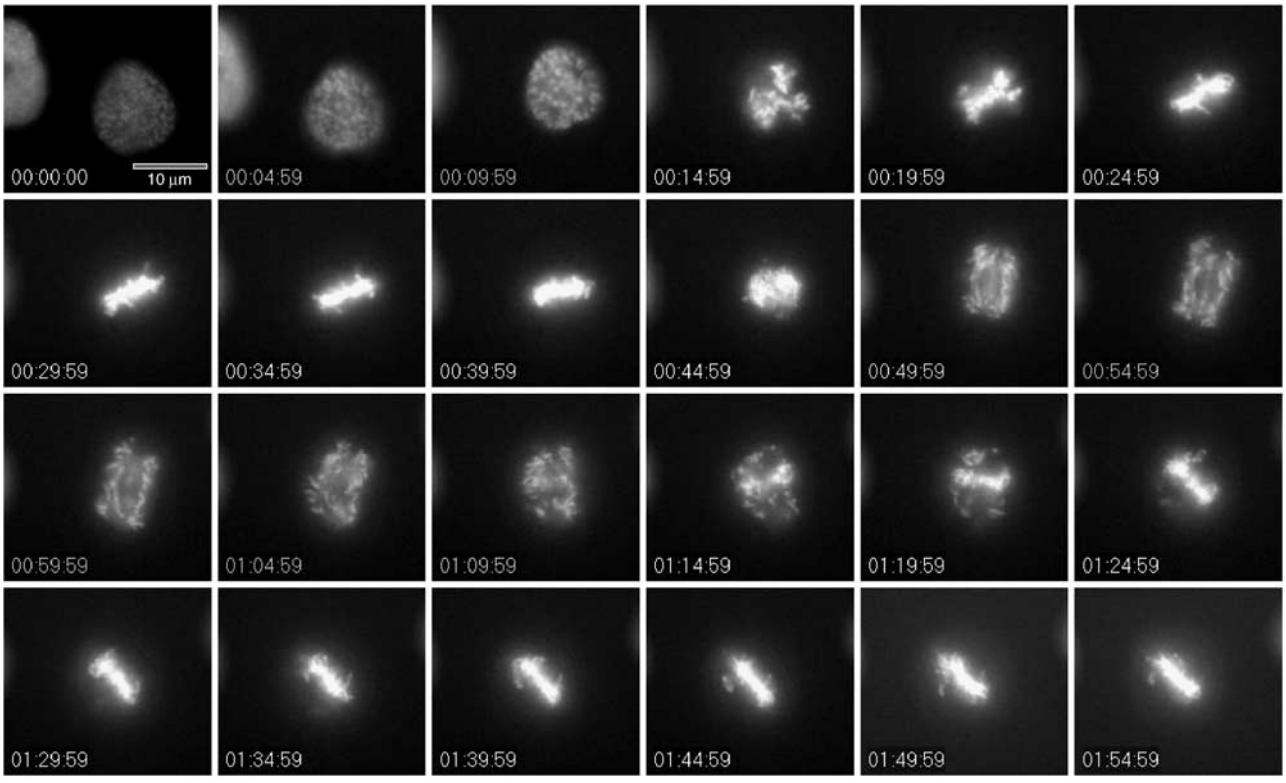

Figure 2 'Pseudometaphase' arrest induced by nondegradable cyclinB1. Onk2-H2B-GFP-mB1NΔ157 cells were synchronised and induced to express mB1NΔ157. Cells about to enter mitosis were filmed using a ×32 objective and images were taken every 2.5 min. For details see text. Time = h:min:s.

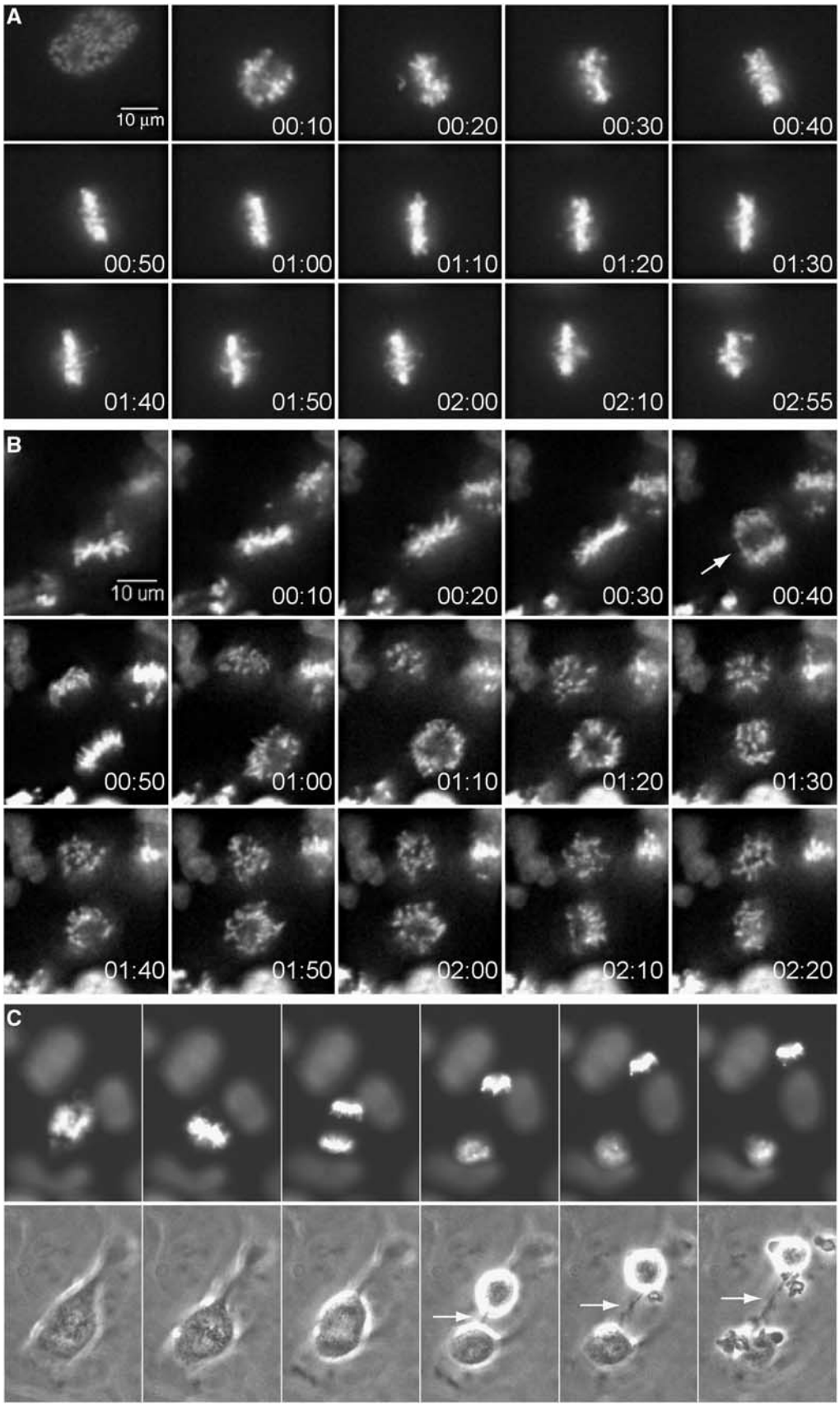

Figure 3 Metaphase and telophase arrest phenotypes induced by nondegradable cyclinB1. (**A**) Synchronised Onk2-H2B-GFP-mB1NΔ157 cells were induced and monitored by time-lapse videomicroscopy as in Figure 2. Selected time frames of a representative cell arrested in metaphase are shown (time = h:min). (**B**) About 22% of arrested cells underwent anaphase (arrow) and initiated cytokinesis, while chromosomes remained condensed. (**C**) A cytoplasmic connection (arrow) remained in cells arrested in telophase.

Table I Nondegradable cyclinB1 arrest phenotypes

Cell line	Arrested cells analysed	Metaphase *n* (%)	Pseudometaphase *n* (%)	Telophase *n* (%)	Other *n* (%)
mB1NΔ157	568	131 (23)	273 (48)	122 (22)	42 (7)
mB1dm	156	29 (19)	106 (68)	21 (13)	—
mB1dmGFP	148	41 (28)	79 (53)	18 (12)	10 (7)

phase to anaphase transition (Figure 2, time frame 10, 45 min after initiation of chromosome condensation), chromosomes first moved away from each other but then congressed again to re-assemble at the equatorial plane. Thus, cells displaying this phenotype apparently entered, but failed to complete, anaphase. The final arrest phenotype after this re-congression of chromosomes was morphologically similar to that of a normal metaphase and stable for several hours with oscillatory chromosome movements readily detectable (see Supplementary Movie 1).

In 23% of cases (Table I, 'metaphase arrest'), cells arrested in mitosis without obvious signs of sister chromatid separation for at least 40 min after the establishment of metaphase. During this prolonged metaphase, or metaphase arrest, we observed that individual chromosomes oscillated significantly in and out of the metaphase plate. After this metaphase arrest, which frequently lasted for several hours (Figure 3A), chromosomes started to lose their position at the cellular equator and became scattered throughout the cell without detectable sister chromatid separation or signs of chromosome decondensation (see Supplementary Movie 2).

In 22% of arrested cells (Table I, 'telophase arrest'), anaphase was readily detectable (white arrow in frame 5 of Figure 3B), but chromosomes remained condensed for several hours (see Supplementary Movie 3). Cytokinesis was initiated in the majority of these cells, which remained connected by a thin cytoplasmic bridge (Figure 3C). Many of these cells re-fused to form a single cell with either two separated sets of condensed chromosomes or chromosomes, which sometimes became re-arranged into a 'pseudometaphase' state (data not shown). Similar results were obtained in mB1dm ($n = 156$) and mB1dm-GFP ($n = 148$) expressing cell lines, in which 19 and 28% arrested in metaphase, 68 and 53% in pseudometaphase and 13 and 12% in telophase, respectively (Table I).

Stable cyclinB1-induced mitotic phenotypes are dose-dependent

To investigate whether the above-described arrest phenotypes might be caused by different expression levels of nondegradable cyclinB1, we induced mB1dm-GFP in cells labelled with histone H2B-mRFP. When we compared GFP signals with the observed phenotypes (Figure 4A), we noted that the highest expression levels were associated with the metaphase arrest (Figure 4A, top row), moderate levels with the pseudometaphase (Figure 4A, middle row) and the lowest levels with the telophase arrest phenotype (Figure 4A, bottom row). Figure 4B shows the GFP levels in cells arrested with the respective phenotypes, while Figure 4C displays the same data by showing the distribution of the three phenotypes in cells grouped according to their GFP levels.

Sister chromatids are separated in pseudometaphase-arrested cells

To assess by an additional method whether and to what extent sister chromatid separation had occurred in cells arrested by nondegradable cyclinB1, we performed chromosome spread analyses of arrested Onk2 cells expressing stable cyclinB1, which had been harvested by mitotic shake-off 24 h after induction. Figure 5A shows representative chromosome spreads of induced Onk2-mB1dm cells in metaphase and anaphase, respectively. We found that more than 90% of arrested cells ($n > 100$) displayed separated sister chromatids (Figure 5C, graph, black bars) and only 10% were arrested in metaphase (white bars). Again, similar results were obtained in mB1NΔ157 expressing cells. These data, thus, confirmed that sister chromatids are truly separated in cells displaying the pseudometaphase phenotype. However, they also argue that defining the arrest phenotypes by live cell timelapse videomicroscopy led to an overestimation of the proportion of cells arrested at metaphase because we could not detect a corresponding fraction of metaphase cells in the chromosome spreads.

To rule out any cell-type specific effect, we transiently transfected H2B-mRFP expressing human HeLa cells with constitutive expression plasmids for wild type and nondegradable cyclin mutants as well as YFP-tagged versions of mouse cyclinB1. Similar to the stably transfected U2OS cell clones described above, chromosomes in the majority of living HeLa cells, arrested in mitosis by nondegradable cyclinB1, appeared as if they were in metaphase (data not shown). To analyse whether sister chromatid separation had occurred in these arrested cells, we performed chromosome spreads 24 h after transfection, which again revealed that more than 80% of HeLa cells displayed separated sister chromatids (black bars).

We concluded from these experiments that nondegradable cyclinB1 at moderate expression levels arrested cells after sister chromatid separation but with chromosomes kept at the equatorial plane. In addition, as endogenous APC/C substrates, such as cyclinB1 and securin, could not be detected in arrested cells (Figure 5C), these data indicate that in cells expressing nondegradable cyclinB1 the APC/C is active, a prerequisite for sister chromatid separation.

Nondegradable cyclinB1 maintains a bipolar 'metaphase-like' spindle

To investigate why anaphase chromosomes assemble near the cellular equator rather than in two separated half-spindles, we analysed mitotic Onk2-mB1dm cells 24 h after induction by staining kinetochores and microtubules using an anticentromere antibody positive serum of a CREST syndrome patient and a α-tubulin specific antibody, respectively. As can be seen in Figure 6A, the mitotic spindle and chromosomes of arrested cells (second row) resembled those

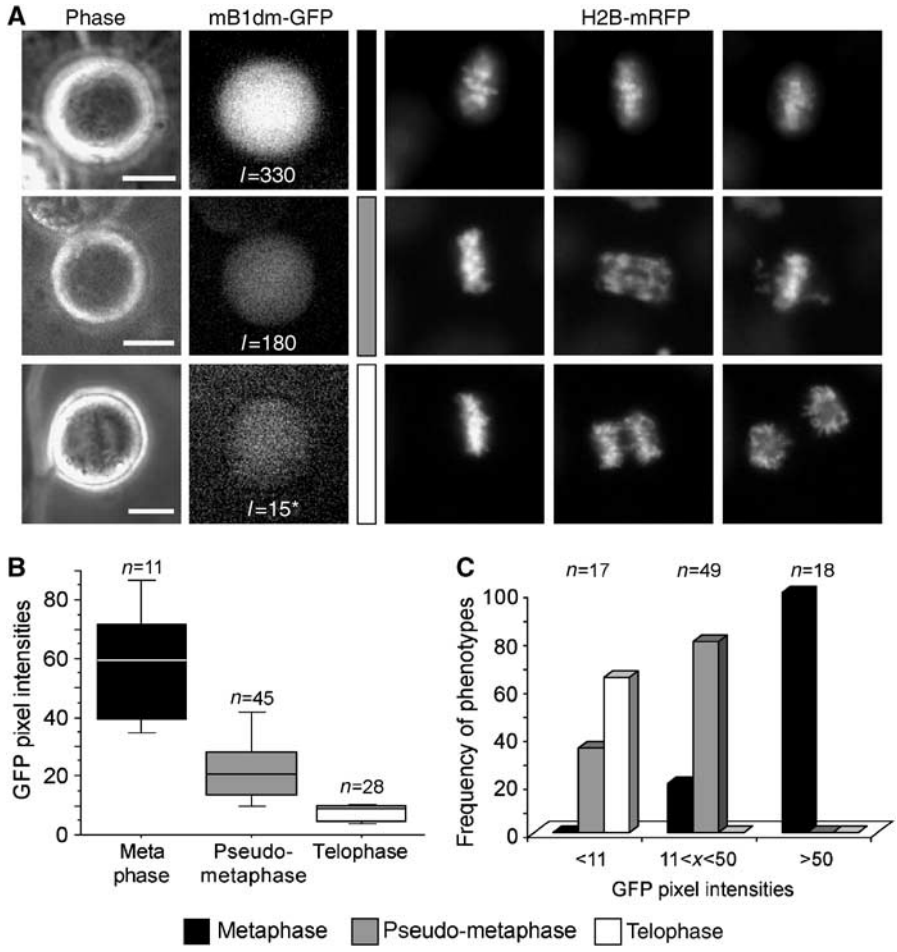

Figure 4 Mitotic arrest phenotypes correlate with cyclinB1 expression levels. (**A**) Onk2 H2B-mRFP mB1dm-GFP cells were induced for 24 h using 1 μg/ml dox and monitored for progression through mitosis by live cell imaging using a × 40 objective. Representative cells with high, medium and low GFP signals and selected corresponding time frames of histone H2B-mRFP recordings are shown. *Image was contrast enhanced to visualise the GFP signal. (B, C) For quantification, cells were monitored using a × 10 objective. The average GFP pixel intensities in cells displaying one of the three cellular arrest phenotypes is shown in (**B**), while the relative frequency of phenotypes in groups of cells displaying similar GFP intensities is shown in (**C**).

of normal metaphases in noninduced cells (top row). In the arrested cell shown, the chromosomes form a broader 'metaphase-like' plate, with chromosomes visible at both spindle poles. Kinetochore staining revealed single kinetochore dots in stable cyclinB1 arrested cells (Figure 6B, lower row), again indicating that sister chromatid separation had occurred. In contrast, normal metaphase cells displayed paired kinetochore dots (Figure 6B, upper row).

To assess the role of microtubules in the 'pseudometaphase' induced by stable cyclinB1, we monitored induced Onk2-H2B-GFP cells expressing mB1NΔ157 until they had 're-assembled' their chromosomes at the cellular equator and added 0.5 μM nocodazole to the media to disrupt microtubules. As can be seen in Figure 6C, 5 min after addition of nocodazole, chromosomes were leaving the equatorial plane and became distributed throughout the cell, suggesting that microtubules were needed to hold the separated sister chromatids in the equatorial plane.

High-resolution time-lapse microscopy of H2B-GFP expressing cells arrested by mB1NΔ157 revealed that individual chromosomes became pulled out of the equatorial zone and remained at the spindle pole until they moved back into the pseudometaphase plate. The majority of chromosomes appeared to be caught and pulled back into the equatorial zone, which caused the chromosomes to bend giving them a U-shaped appearance (Figure 7A, top panel, Supplementary Movie 4). In some cases, chromosomes could be detected which moved towards the equatorial zone as stretched chromosomes (Figure 7A, lower panel, Supplementary Movie 5). We envisaged two possible explanations for this phenotype (see Figure 7B): (1) merotelic attachment of individual chromosomes, that is, attachment of a single kinetochore to both spindle poles, and (2) maintenance of a strong 'polar wind', or polar ejection force, able to push chromosomes away from the poles into the middle of the cell. To look for merotelic attachment, we selectively stained kinetochore-bound microtubules (Mitchison *et al*, 1986) and kinetochores using CREST antisera, which revealed that most of the kinetochores were attached monotelically, that is, to one spindle pole only (arrows, Figure 7C), while some kinetochores appeared to be merotelically attached (arrowhead).

We speculated that if chromosomes were merotelically attached, they might interfere with the formation of the central spindle and cytokinesis. To test this hypothesis, we treated cells arrested by nondegradable cyclinB1 with 20 μM R-roscovitine, which triggered cytokinesis within 10 min

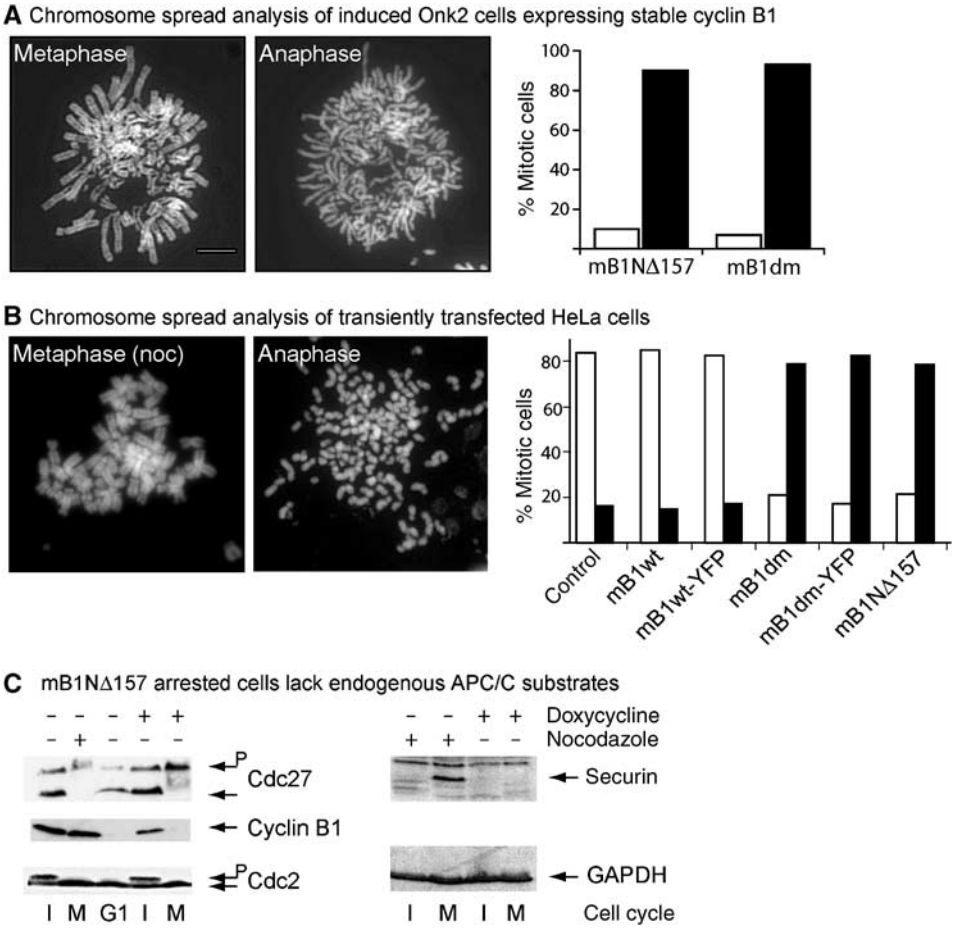

Figure 5 Sister chromatid separation in cells arrested with nondegradable cyclinB1. (**A**) Mitotic Onk2 mB1dm cells were harvested 24 h after induction and analysed by chromosome spreading. One metaphase cell and one cell arrested in anaphase are shown. Size bar indicates 5 μm. The bar graph shows a summary of mB1dm and mB1NΔ157 cells induced for 24 h and analysed by chromosome spreading. White bars = metaphase cells; black bars = anaphase cells ($n > 100$ in both cell lines). (**B**) Chromosome spread analysis of transiently transfected mitotic HeLa cells. A cell arrested at metaphase by nocodazole treatment for 16 h is shown as a control. A representative chromosome spread of a HeLa cells transfected with mB1dm is shown (anaphase). The bar graph summarises experiments using HeLa cells that were transiently transfected with the indicated plasmids ($n > 100$ for each transfection experiment). (**C**) Left panel: Total cell extracts from adherent interphase (I) or mitotic (M) Onk2-mB1NΔ157 cells that were either left untreated (lanes 1 and 4), nocodazole treated (0.5 μM, 16 h, lane 2), 4 h released from a 16 h nocodazole block (lane 3), or dox-treated (lanes 4 and 5) were analysed for Cdc27, cyclin B1 and Cdc2. G1 = G1 phase. Right panel: total cell extracts from nonmitotic (lane 1) and mitotic (lane 2) nocodazole-treated as well as nonmitotic (lane 3) and mitotic dox-induced (lane 4) mB1NΔ157 cells were analysed for securin and GAPDH expression by immunoblotting.

($n = 23$) after addition of the kinase inhibitor. In contrast to the rapid onset of cytokinesis, anaphase chromosome movements could not be restored. Frequently, a set of chromosomes remained in the middle of the cells and prevented completion of cytokinesis, indicating that they might be attached to both spindle poles (Figure 7D). These data suggest that merotelic attachment might contribute to the arrest phenotype by capturing chromosomes at the poles and pulling them back into the equatorial zone, but that merotelic attachment might not be stable enough to hold all chromosomes in this pseudometaphase plate.

The chromokinesin hKid is required for chromosome re-alignment in anaphase arrested cells

To investigate whether the polar ejection force might contribute to the pseudometaphase phenotype, we probed the function of the chromokinesin hKid, a major contributor to the so-called 'polar wind' that is expressed in cells arrested by nondegradable cyclinB1 (Figure 8A) by RNA interference (RNAi) to knockdown hKid in human cells. As can be seen in Figure 8B, transfection of Onk2 cells (transfection efficiency 70%) with siRNAs directed against hKid caused a significant reduction of hKid in induced as well as non-induced cells. To investigate the role of hKid in cyclinB1 arrested cells, Onk2 cells were transfected with hKid siRNAs for 6 h and induced to express nondegradable cyclin mB1NΔ157 for 24 h. As summarised in Figure 8B (right panel), transfection of hKid specific siRNAs (grey bars), but not control siRNAs (white bars), prevented the stable re-assembly of separated anaphase chromosomes into a second 'metaphase-like' structure (see Supplementary Movie 6). Of 120 arrested cells analysed (Figure 8B), 29% behaved like control cells as they re-aligned their chromosomes after visible onset of anaphase, while ~60% failed to re-align their chromosomes at the metaphase plate and arrested in anaphase or telophase. Induced mB1NΔ157 cells transfected with nonfunctional siRNAs behaved like mock- or nontransfected cells.

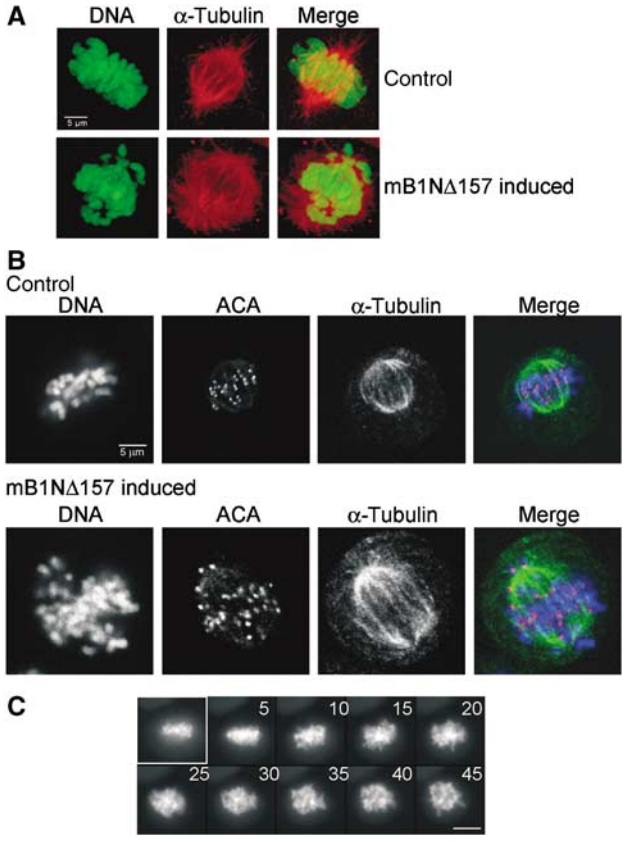

Figure 6 The mitotic spindle is maintained in arrested cells. (**A**) Like control cells (top row), arrested cells contain a bipolar spindle as visualised by staining of methanol fixed mB1NΔ157 expressing Onk2-H2B-GFP cells for α-tubulin (Tat-1, Alexa546). (**B**) Kinetochores are not paired in Onk2 mB1dm arrested cells (2nd row): kinetochores were stained using an anticentromere antibody (ACA) positive CREST serum (FITC) in combination with α-tubulin (Alexa546) staining in Onk2-H2B-GFP cells expressing nondegradable cyclinB1. Confocal images were taken at 1 μm *z*-sections. (**C**) Induced H2B-GFP expressing Onk2-mB1NΔ157 arrested cells were monitored to undergo anaphase and re-assemble their chromosomes at the cellular equator, then treated with 0.5 μM nocodazole and followed by fluorescence time-lapse video-microscopy ($n=4$). Time after addition of nocodazole is shown in min. Size bar is 10 μm.

To confirm these findings by a second technique, we employed microinjection of neutralising anti-hKid antibodies (Levesque and Compton, 2001) into synchronised and induced mB1NΔ157 cells. As exemplified in Figure 8C, microinjection of neutralising anti-hKid antisera in G2-phase cells, prevented the re-assembly of separated chromosomes in all of 58 successfully injected and mB1NΔ157-arrested cells. The right panel in Figure 8C shows a representative noninjected cell from the same experiment displaying the 'pseudometaphase' arrest phenotype. Control microinjection experiments (dye alone or control antibodies) had no effect on the 're-assembly' of anaphase chromosomes into a second 'metaphase-like' state (data not shown).

Taken together, we concluded from these experiments that expression of nondegradable cyclinB1 arrested cells after sister chromatid separation but prevented anaphase chromosome movements. Surprisingly, the chromosomes in these cells re-aligned at the cellular equator, a phenomenon dependent on the chromokinesin hKid. To examine whether hKid controls chromosome positioning in cells arrested in anaphase by another mechanism, we assessed chromosome dynamics in Sgo1-RNAi cells, which arrest in mitosis due to the activation of the spindle assembly checkpoint by the precociously separated sister chromatids (Salic *et al*, 2004). Arrested Sgo1 knockdown cells are, thus, similar to cells arrested by nondegradable cyclinB1 except that the APC/C is inactive in the former but active in the latter. U2OS-H2B-mRFP cells transfected with Sgo1 specific siRNAs (Salic *et al*, 2004) arrested in mitosis with chromosomes aligned at the cellular equator for several hours (mean = 195 min, $n=18$) before chromosomes became scattered throughout the cells. Co-depletion of hKid by RNAi caused a significant change in chromosome localisation since in 80% of double RNAi cells ($n=26$), chromosomes started to become scattered earlier (mean = 65 min) than in Sgo1 only RNAi cells (Supplementary Figure S2 and Supplementary Movies 7 and 8). Thus, in Sgo1 knockdown cells, similar to cells arrested by nondegradable cyclinB1, hKid is required to keep chromosomes near the cellular equator.

In summary, our data suggest that the destruction of cyclinB1 during mitosis is not required for sister chromatid separation in human cells but is required for normal anaphase chromosome movements, a process that appears to depend on the chromokinesin hKid.

Discussion

The multiple roles of Cdk1 during mitosis have been compared to traffic lights, since Cdk1 promotes many early mitotic events and, at the same time, inhibits several late mitotic processes by phosphorylation and direct binding, which reverses at the onset of anaphase, when cyclinB1 degradation starts (Nasmyth, 2001a). Cdk1 inactivation requires cyclinB1 degradation for exit from mitosis but which of the processes that follow metaphase depend on cyclinB1 proteolysis are still not elaborated at the molecular level. CyclinB1 degradation has been linked to the regulation of sister chromatid separation by revealing a direct inhibitory effect of the cyclinB1/Cdk1 complex on the activity of separase activity *in vitro* (Stemmann *et al*, 2001; Gorr *et al*, 2005). In contrast to this direct inhibitory mechanism, inhibition of cytokinesis has been linked to the failure to form a spindle midzone during ana- and telophase (Wheatley *et al*, 1997) although more direct inhibitory effects on regulators of cytokinesis might be operative as well.

In order to determine which mitotic processes are dependent on cyclinB1 proteolysis, we generated a panel of human cell lines with conditional expression of nondegradable cyclinB1. To quantify transgene expression levels, we used cyclinB1-GFP intensities to compare them with total cyclinB1 levels. These analyses revealed that cyclinB1 accumulated to approximately two- to three-fold higher levels in the majority of the induced cells. Since the APC/C was active in cells arrested by stable cyclinB1, endogenous cyclinB1 became degraded and the cells arrested with transgenic stable cyclinB1 levels that were close to endogenous cyclinB1 levels at metaphase. The expression levels achieved using stable inducible cell lines thus provided a good model system to study the role of cyclinB1 degradation during mitosis.

When Onk2-H2B-GFP cells were induced to express nondegradable cyclinB1, we noticed a high frequency of mito-

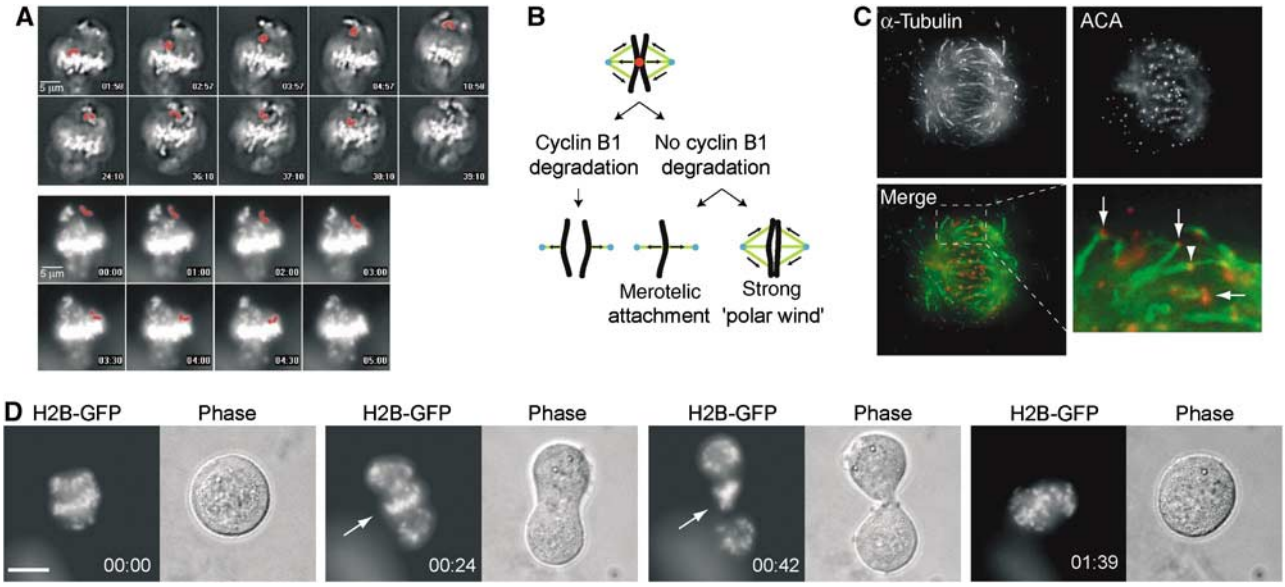

Figure 7 Merotelic kinetochore attachment in cells arrested by nondegradable cyclinB1. (**A**) Images of H2B-GFP signals of induced mB1NΔ157 cells were taken in 30 s. intervals using a ×40 objective. Shown are selected time frames of Supplementary Movie 4 with the elapsed time indicated in min:s. A chromosome discussed in the text is highlighted by red pseudocoloring. The lower panel shows an oscillating, slower moving, chromosome, which does not change its shape as it moves back (Supplementary Movie 5). (**B**) Model for the metaphase-like arrangement of anaphase chromosomes in stable cyclinB1 arrested cells. In the absence of cyclinB1 degradation, separated sister chromatids might achieve a metaphase-like arrangement by merotelic attachment, a 'strong polar wind' or by a combination of both. (**C**) Kinetochore microtubule bundles (α-tubulin) and kinetochores (ACA = CREST) were stained after selective depletion of nonkinetochore microtubules and are shown as maximum projections of deconvolved 0.5 μm *z*-series taken with a ×63 objective. The bottom row shows the overlay of the α-tubulin and kinetochore stainings and an enlarged area to highlight monotelically (arrows) as well as merotelically attached (arrowhead) kinetochores. (**D**) mB1NΔ157 induced arrested cells were treated with 20 μM R-roscovitine and followed by live cell imaging. The selected cell shown attempts a futile cytokinesis, which appears to be blocked by nonsegregating chromatin remaining in between the middle of the cell (arrow). Size bar = 10 μm. Time = h:min.

tically arrested cells that were apparently in metaphase. However, when we analysed chromosome behaviour in living arrested cells, we discerned three mitotic phenotypes, two of which displayed sister chromatid separation. In one of those, that is, the 'pseudometaphase' phenotype, however, chromosomes re-congressed to the cellular equator causing a terminal phenotype similar to truly metaphase arrested cells. Thus, while in end point analysis, the majority of cells appeared as if arrested at metaphase, time-lapse videomicroscopy revealed that the majority of cells arrested in anaphase, which could be confirmed by chromosome spread analysis.

By correlating the cyclinB1-GFP signals with endogenous cyclinB1 levels in immunostaining experiments, we have shown that, in highly mB1dm-GFP positive mitotic cells, a three to four times higher total cyclinB1 content could be detected than in nocodazole-treated noninduced control cells. This amount of nondegradable cyclinB1 apparently kept cells in metaphase, as judged by time-lapse videomicroscopy. However, since we failed to detect a corresponding fraction of metaphases in chromosome spreads, we suspect that in our system high levels of nondegradable cyclinB1 only caused a partial inhibition of sister chromatid separation.

In the majority of cells that expressed mB1dm-GFP at levels similar to endogenous cyclin B1 levels in noninduced nocodazole-treated control cells, anaphase was not blocked, consistent with biochemical data, showing that only high levels of cyclinB1/Cdk1 levels are able to block the onset of anaphase (Stemmann *et al*, 2001). Our data are, however, in contrast to previously published observations claiming that low amounts of nondegradable cyclinB1 are sufficient to arrest human cells in metaphase. In their study, Chang *et al* (2003) have found that stable cyclinB1 affects the recovery, that is, the onset of anaphase, of cells released from a nocodazole block, while we and others (Hagting *et al*, 2002) have studied the effects of stable cyclinB1 in an unperturbed mitosis. Interestingly, Gorr *et al* (2005) have recently discovered that cyclin B1/Cdk1 and securin bind to and inhibit separase in a mutually exclusive manner *in vitro*, suggesting that a prolonged mitotic arrest, for example, caused by nocodazole treatment, might allow the formation of inactive cyclinB1/Cdk1/separase complexes.

We have focused on the effects of moderate levels overexpression levels of nondegradable cyclinB1, which did not block sister chromatid separation but otherwise maintained many aspects of metaphase, such that anaphase chromosomes became arranged into a 'metaphase-like' state by a bipolar spindle. This mitotic arrest phenotype is specific for nondegradable cyclinB1, as nondegradable cyclin A arrested cells in anaphase without forming a 'metaphase-like' arrangement of chromosomes (Geley *et al*, 2001). To explain how separated sister chromatids can re-align at the cellular equator—like during normal prometaphase—we have investigated whether chromosomes return to, and are kept at, the cellular equator by the action of the chromokinesin hKid and/or by the merotelic attachment of individual kinetochores.

The chromokinesin Kid is a plus end-directed motor protein (Yajima *et al*, 2003) that, in human mitosis, is responsible for a considerable part of the polar ejection force (Levesque and Compton, 2001; Brouhard and Hunt, 2005) and that is required for chromosome congression in spindles formed

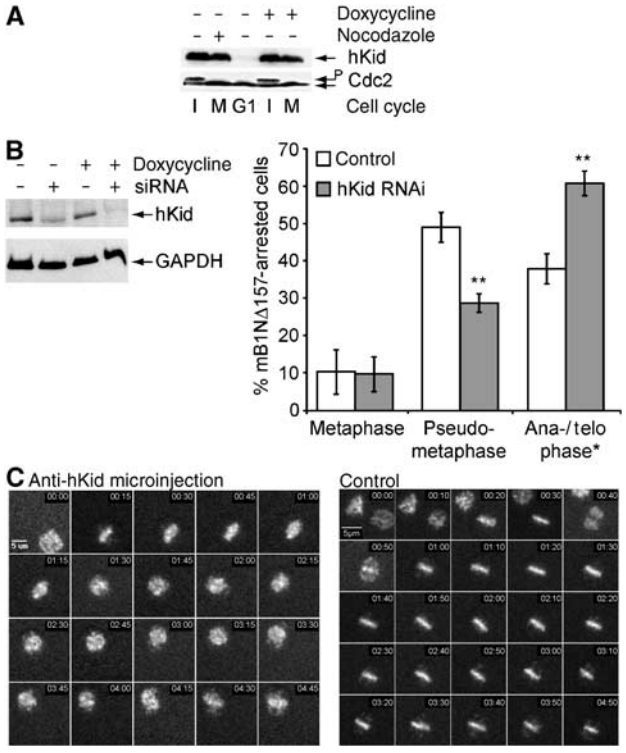

Figure 8 (**A**) hKid is required for the metaphase-like reassembly of anaphase chromosomes in arrested cells. hKid is expressed in cells arrested by nondegradable cyclinB1 (legend as in Figure 5C). Cdc2 levels are shown as loading controls. (**B**) hKid RNAi. Onk2 cells were transfected with 50 nM hKid siRNAs for 6 h, induced to express cyclin mB1NΔ157 for 24 h and monitored by time-lapse videomicroscopy. At 26 h after transfection, cells were harvested and analysed for hKid protein expression (left panel). Right panel: Summary of time-lapse analysis of induced mB1NΔ157 cells transfected with hKid specific (grey bars) or nonspecific siRNAs (white bars). Progression through mitosis was monitored by observing H2B-GFP signals in more than 200 cells over more than 12 h by fluorescence time-lapse videomicroscopy. Shown are the frequencies of mitotic phenotypes of one out of three independent experiments with similar results (**t-test $P<0.001$). (**C**) Synchronised and induced Onk2-H2B-GFP mB1NΔ157 expressing cells were microinjected with affinity purified rabbit antiserum (10 mg/ml) directed against the DNA binding domain of hKid and followed by time-lapse video microscopy using a $\times 10$ objective. Injected cells were identified by co-injected Rhodamine-labelled dextran. The representative cell shown (left panel) enters mitosis and after the onset of anaphase displays rapidly moving scattered chromosomes. The majority (>50%) of noninjected cells (a representative cell is shown in the right panel) displayed the pseudometaphase arrest. Time = h:min.

in cell-free extracts derived from *Xenopus* eggs (Antonio *et al*, 2000; Funabiki and Murray, 2000). Inactivation or down-regulation of hKid, by antibody microinjection and RNAi, respectively, prevented the major stable cyclinB1 arrest phenotype, that is, pseudometaphase and, thus, seemed to be required to form a stable bipolar spindle in these anaphase arrested cells. However, in cells displaying the 'pseudometaphase' phenotype, chromosomes first separate from each other before they congress again, suggesting that the 'polar wind' is not sufficient to keep chromosomes at the cellular equator in anaphase arrested cells. Therefore, we investigated whether anaphase chromosomes might have regained bipolar, that is, merotelic, attachment of individual kinetochores. By selectively staining for kinetochore microtubules and kinetochores, we could detect merotelically attached individual kinetochores, although the majority of kinetochores in cells arrested by nondegradable cyclinB1 was attached to one spindle pole only. As survivin and Aurora B kinase, known regulators of the attachment of microtubules to kinetochores (Tanaka *et al*, 2002; Lampson *et al*, 2004), remained kinetochore-bound in arrested cells (unpublished data), kinetochore–microtubule interactions might be unstable consistent with the observed oscillatory behaviour of anaphase chromosomes in cells arrested by nondegradable cyclinB1. Our data support the hypothesis that stable cyclinB1 maintains kinetochores in a (pro)metaphase-like state, similar to results obtained in *Drosophila* embryos expressing nondegradable cyclinB (Parry *et al*, 2003).

Under conditions where bipolar chromosome attachment is impaired or unstable, like in cells arrested in anaphase by nondegradable cyclinB1 or Sgo1 RNAi, hKid seems to play an important role in chromosome positioning and is required to maintain a bipolar spindle. In contrast, hKid does not seem to play an essential role in chromosome congression during normal mitosis (Levesque and Compton, 2001), suggesting that bipolar chromosome attachment and chromosome congression is controlled by multiple redundant pathways. In cells arrested by nondegradable cyclinB1, two properties of prometaphase cells are maintained, that is, the capacity to establish microtubule–kinetochore interactions and the expression of the chromokinesin hKid. Our analysis, thus, suggests that cyclinB1 inactivation during mitosis is either required to switch off the microtubule binding capacity of kinetochores or is required to allow efficient poleward movement of the chromosomes, for example, by turning off the chromokinesin hKid.

The third class of mitotic arrest phenotype, that is, 'telophase' arrest, was caused by the lowest expression levels of mB1dm-GFP. In most of these arrested cells, the onset of cytokinesis was not blocked but cells remained connected via a cytoplasmic bridge. In all of the arrested cells, chromosomes remained condensed suggesting that the final stages of mitosis, including chromosome decondensation and cellular abscission might require the complete inactivation of cyclinB1/Cdk1.

By studying the relationship between expression levels of nondegradable cyclinB1 and mitotic arrest phenotypes determined by live cell imaging of histone H2B-GFP tagged chromosomes, we have found that high levels of stable cyclinB1 appeared to delay sister chromatid separation, while more moderate overexpression of nondegradable cyclinB1 did not block anaphase. Surprisingly, stable cyclinB1 maintained a bipolar spindle, with anaphase chromosomes positioned near the cellular equator. In addition, this pseudometaphase phenotype was characterised by merotelic attachment of anaphase chromosomes and required the chromokinesin hKid. As low levels of stable cyclinB1 only block the final stages of mitosis, such as cellular abscission and chromosome decondensation, these data suggest that the decline of Cdk1 activity after the onset of anaphase might set thresholds that control progression through the final steps of mitosis.

Materials and methods

The online supplementary file contains additional information about the reagents and methods used in this study.

Reagents, plasmids and antibodies

All chemicals were obtained from Sigma (Vienna, Austria), enzymes from Promega (Mannheim, Germany) and oligonucleotides from MWG Biotech (Ebersberg, Germany), unless stated otherwise. Wild-type, truncation and D-box mutants of mouse cyclinB1 and GFP-tagged cyclinB1 were generated by PCR using plasmids pEF-mB1, pEF-mB1dm and pEF-mB1-GFP (M Brandeis, Jerusalem, Isreal) as templates (Geley *et al*, 2001), subcloned into pEFΔT (unpublished) or pUHD10-3, for constitutive and tetracycline inducible expression, respectively. CyclinB1-YFP fusion constructs have been described (Pepperkok *et al*, 1999). Retroviral expression constructs for histone H2B-fusion proteins were obtained by cloning H2B-GFP and H2B-mRFP into pLib-ires-Puro and pLib-ires-BlaS (M Ausserlechner, Innsbruck, Austria), respectively.

The following antibodies were used: cyclinB1 (mAb V152), mouse cyclinB1 (mAb V143), α-tubulin (mAb TAT-1), Cdk1 (mAb A17, J Gannon, South Mimms, UK), human CREST serum (G Wick, Innsbruck), hKid-DBD (rb, DNA-binding domain) and hKid-N (rb, neck region of motor domain, both D Compton, Hanover, USA), hKid mAb 8C12 (Wandke and Geley, 2006), Cdc27 (mAb, BD Transduction, Vienna, Austria), Sgo1 (rb, A Salic, Boston, USA) and securin (rb, J-M Peters, Vienna). For immunofluorescence, AlexaFluor 488,546 (Invitrogen, Lofer, Austria) and FITC- or TRITC-labelled appropriate secondary antibodies were used.

Cell culture, transfection and retroviral transduction

Onk2, HeLa cells and the Phoenix amphotropic packaging cell line (G Nolan, Stanford, USA) were grown as described (Geley *et al*, 2001; Ausserlechner *et al*, 2004). For live-cell imaging or immunofluorescence staining experiments, cells were grown on glass-bottomed dishes. Cell cycle synchronisation was performed using a double thymidine block as described (Geley *et al*, 2001). For transient transfection experiments, Lipofectamine 2000 (Invitrogen) was used according to the manufacturers' protocols; stable transfection was carried out as described (Geley *et al*, 2001). VSV-G pseudotyped retroviral particles were generated by transfection of Phoenix cells with pLib-based plasmids and pMD.G (M Collins, London, UK) and used to infect Onk2 and HeLa cells as described (Ausserlechner *et al*, 2004). Selection of transduced cells was performed using 2.5 μg/ml Puromycin or 5 μg/ml Blasticidin S (Calbiochem, VWR International). Onk2 cells were used to generate inducible mB1wt, mB1dm, mB1- and mB1dm-GFP clones. Strongly inducible Onk2-mB1dm and -mB1dm-GFP clones were transduced with retroviruses expressing histone H2B-GFP and H2B-RFP, respectively. Onk2-H2B-GFP cells were used to generate inducible mB1NΔ157 cells.

Immunoblotting and immunofluorescence

Immunoblotting was performed as described (Geley *et al*, 2001) and membranes either developed using ECL (Amersham) or infrared detection and quantification using an Odyssey system (Li-Cor Biosciences, Bad Homburg, Germany). ECL-autoradiographs were scanned, calibrated and quantified using ImageJ (Abramoff *et al*, 2004). For immunofluorescence staining, cells were processed as described (Geley *et al*, 2001). To selectively visualise kinetochore microtubules, cells were pre-extracted with 0.5% Triton X-100/0.1 mM $CaCl_2$ for 60–90 s followed by fixation in 3.7% paraformaldehyde. For chromosome spreads, cells were harvested by mitotic shake off, resuspended in 0.56% w/v KCl and incubated for 15 min. Pelleted cells were carefully resuspended in Carnoy's fixative (75% methanol, 25% acetic acid) for 20 min, washed twice in fixative, resuspended in 200–500 μl fixative and dropped onto a slide. Finally, air dried chromosomes were stained with 1 μg/ml Hoechst 33342.

Live cell video-microscopy, image acquisition and processing

Live cell microscopy was performed on an Axiovert 200 M microscope (Carl Zeiss, Jena, Germany) equilibrated to 37°C and equipped for live cell imaging. Images were taken using a CoolSnap*fx* camera (Roper Scientific, Ottobrunn, Germany) controlled by Metamorph software 5.0 (Molecular Devices, Downington, USA). For high-resolution microscopy and 3D reconstructions, serial 0.3–1 μm *z*-sections in each wavelength were acquired with a Plan Apochromat ×63 1.4NA or ×100 1.45NA objective and *z*-stacks deconvolved using Autodeblur software (AutoQuant). Confocal images were generated on an Axiovert 100 LSM510 microscope using a ×63 objective. GFP fluorescence intensities were quantified by determining average pixel values over cell areas after background correction. Image processing was first performed in Metamorph and after conversion to 8-bit TIFF images continued using Photoshop7.0 and Illustrator10 (Adobe).

Microinjection and RNA interference

Microinjection of induced G2-phase Onk2-mB1NΔ157 cells was performed using an Eppendorf InjectMan and FemtoJet microinjection unit (Eppendorf, Vienna) as described (Geley *et al*, 2001). For RNAi, 25–50 nM of specific or control siRNA (hKid, 5′CAAGCUCAC UCGCCUAUUGdTdT) were transfected using Lipofectamine 2000.

Supplementary data

Supplementary data are available at *The EMBO Journal* Online.

Acknowledgements

We thank L Sparber for excellent technical assistance, C Ploner and H Niederegger for their help, M Ausserlechner, M Brandeis, M Collins, D Compton, J Gannon, T Hunt, G Nolan, J-M Peters, A Salic, R Tsien, G Wick for essential reagents, A Helmberg and R Kofler for critically reading the manuscript. This work was supported by Grants P15000 and P16400-B10 from the Austrian Science Funds (FWF) as well as by an FWF Special Research Program (SFB021, 'Cell death and proliferation in tumours') and EU Grant LSHS-CT-2004-503438 ('TRANSFOG').

References

Abramoff MD, Magelhaes PJ, Ram SJ (2004) Image processing with Image J. *Biophotonics Int* **11:** 36–42

Antonio C, Ferby I, Wilhelm H, Jones M, Karsenti E, Nebreda AR, Vernos I (2000) Xkid, a chromokinesin required for chromosome alignment on the metaphase plate. *Cell* **102:** 425–435

Ausserlechner MJ, Obexer P, Bock G, Geley S, Kofler R (2004) Cyclin D3 and c-MYC control glucocorticoid-induced cell cycle arrest but not apoptosis in lymphoblastic leukemia cells. *Cell Death Differ* **11:** 165–174

Brouhard GJ, Hunt AJ (2005) Microtubule movements on the arms of mitotic chromosomes: polar ejection forces quantified *in vitro*. *Proc Natl Acad Sci USA* **102:** 13903–13908

Chan GK, Yen TJ (2003) The mitotic checkpoint: a signaling pathway that allows a single unattached kinetochore to inhibit mitotic exit. *Prog Cell Cycle Res* **5:** 431–439

Chang DC, Xu N, Luo KQ (2003) Degradation of cyclin B is required for the onset of anaphase in mammalian cells. *J Biol Chem* **278:** 37865–37873

Clute P, Pines J (1999) Temporal and spatial control of cyclin B1 destruction in metaphase. *Nat Cell Biol* **1:** 82–87

Funabiki H, Murray AW (2000) The *Xenopus* chromokinesin Xkid is essential for metaphase chromosome alignment and must be degraded to allow anaphase chromosome movement. *Cell* **102:** 411–424

Gallant P, Nigg EA (1992) Cyclin B2 undergoes cell cycle-dependent nuclear translocation and, when expressed as a non-destructible mutant, causes mitotic arrest in HeLa cells. *J Cell Biol* **117:** 213–224

Geley S, Kramer E, Gieffers C, Gannon J, Peters JM, Hunt T (2001) Anaphase-promoting complex/cyclosome-dependent proteolysis of human cyclin A starts at the beginning of mitosis and is not subject to the spindle assembly checkpoint. *J Cell Biol* **153:** 137–148

Gorr IH, Boos D, Stemmann O (2005) Mutual inhibition of separase and Cdk1 by two-step complex formation. *Mol Cell* **19:** 135–141

Hagting A, den Elzen N, Vodermaier HC, Waizenegger IC, Peters JM, Pines J (2002) Human securin proteolysis is controlled by the

spindle checkpoint and reveals when the APC/C switches from activation by Cdc20 to Cdh1. *J Cell Biol* **157:** 1125–1137

Herbert M, Levasseur M, Homer H, Yallop K, Murdoch A, McDougall A (2003) Homologue disjunction in mouse oocytes requires proteolysis of securin and cyclin B1. *Nat Cell Biol* **5:** 1023–1025

Holloway SL, Glotzer M, King RW, Murray AW (1993) Anaphase is initiated by proteolysis rather than by the inactivation of maturation-promoting factor. *Cell* **73:** 1393–1402

Jallepalli PV, Waizenegger IC, Bunz F, Langer S, Speicher MR, Peters JM, Kinzler KW, Vogelstein B, Lengauer C (2001) Securin is required for chromosomal stability in human cells. *Cell* **105:** 445–457

Lampson MA, Renduchitala K, Khodjakov A, Kapoor TM (2004) Correcting improper chromosome-spindle attachments during cell division. *Nat Cell Biol* **6:** 232–237

Levesque AA, Compton DA (2001) The chromokinesin Kid is necessary for chromosome arm orientation and oscillation, but not congression, on mitotic spindles. *J Cell Biol* **154:** 1135–1146

Madgwick S, Nixon VL, Chang HY, Herbert M, Levasseur M, Jones KT (2004) Maintenance of sister chromatid attachment in mouse eggs through maturation-promoting factor activity. *Dev Biol* **275:** 68–81

McGuinness BE, Hirota T, Kudo NR, Peters JM, Nasmyth K (2005) Shugoshin prevents dissociation of cohesin from centromeres during mitosis in vertebrate cells. *PLoS Biol* **3:** e86

Mitchison T, Evans L, Schulze E, Kirschner M (1986) Sites of microtubule assembly and disassembly in the mitotic spindle. *Cell* **45:** 515–527

Nasmyth K (2001a) A prize for proliferation. *Cell* **107:** 689–701

Nasmyth K (2001b) Disseminating the genome: joining, resolving, and separating sister chromatids during mitosis and meiosis. *Annu Rev Genet* **35:** 673–745

Parry DH, Hickson GR, O'Farrell PH (2003) Cyclin B destruction triggers changes in kinetochore behavior essential for successful anaphase. *Curr Biol* **13:** 647–653

Pepperkok R, Squire A, Geley S, Bastiaens PI (1999) Simultaneous detection of multiple green fluorescent proteins in live cells by fluorescence lifetime imaging microscopy. *Curr Biol* **9:** 269–272

Peters JM (2002) The anaphase-promoting complex: proteolysis in mitosis and beyond. *Mol Cell* **9:** 931–943

Salic A, Waters JC, Mitchison TJ (2004) Vertebrate shugoshin links sister centromere cohesion and kinetochore microtubule stability in mitosis. *Cell* **118:** 567–578

Stemmann O, Zou H, Gerber SA, Gygi SP, Kirschner MW (2001) Dual inhibition of sister chromatid separation at metaphase. *Cell* **107:** 715–726

Tanaka TU, Rachidi N, Janke C, Pereira G, Galova M, Schiebel E, Stark MJ, Nasmyth K (2002) Evidence that the Ipl1-Sli15 (Aurora kinase-INCENP) complex promotes chromosome bi-orientation by altering kinetochore–spindle pole connections. *Cell* **108:** 317–329

Waizenegger I, Gimenez-Abian J, Wernic D, Peters J (2002) Regulation of human separase by securin binding and autocleavage. *Curr Biol* **12:** 1368

Wandke C, Geley S (2006) Generation and characterization of an hKid specific monoclonal antibody. *Hybridoma* **25:** 41–43

Wheatley SP, Hinchcliffe EH, Glotzer M, Hyman AA, Sluder G, Wang Y (1997) CDK1 inactivation regulates anaphase spindle dynamics and cytokinesis *in vivo*. *J Cell Biol* **138:** 385–393

Yajima J, Edamatsu M, Watai-Nishii J, Tokai-Nishizumi N, Yamamoto T, Toyoshima YY (2003) The human chromokinesin Kid is a plus end-directed microtubule-based motor. *EMBO J* **22:** 1067–1074

Zur A, Brandeis M (2001) Securin degradation is mediated by fzy and fzr, and is required for complete chromatid separation but not for cytokinesis. *EMBO J* **20:** 792–801